

The Effects of Dynamic Vulcanization and Compatibilizer on Properties of Paper Sludge-Filled Polypropylene/Ethylene Propylene Diene Terpolymer Composites

H. Salmah,¹ H. Ismail,² A. Abu Bakar²

¹*School of Materials Engineering, Northern Malaysia University College of Engineering (KUKUM), 02600 Jejawi, Perlis, Malaysia*

²*School of Materials and Mineral Resources Engineering, Universiti Sains Malaysia, 14300 Nibong Tebal, Penang, Malaysia*

Received 28 June 2005; accepted 9 February 2007

DOI 10.1002/app.27367

Published online 6 November 2007 in Wiley InterScience (www.interscience.wiley.com).

ABSTRACT: The effects of dynamic vulcanization (DV) and dynamic vulcanization plus compatibilizer (DVC) of paper sludge (PS) filled polypropylene/ethylene propylene diene terpolymer (PP/EPDM) composites on torque development, mechanical properties, water absorption, morphology, and thermal properties were studied. Results show that DV and DVC composites exhibit higher stabilization torque than unvulcanized composites (UV). The dynamic vulcanized (DV) and dynamic vulcanized plus compatibilizer (DVC) composites exhibit higher tensile strength, elongation at break, and Young's modulus but lower water absorption

than unvulcanized composites. The scanning electron microscopy (SEM) study of tensile fracture surface of DV and DVC composites shows the improved interfacial interaction between PS and PP/EPDM matrix. The DV and DVC composites also exhibit better thermal stability and higher crystallinity than unvulcanized PP/EPDM/PS composites. © 2007 Wiley Periodicals, Inc. *J Appl Polym Sci* 107: 2266–2273, 2008

Key words: dynamic vulcanization; compatibilizer; paper sludge; polypropylene; ethylene propylene diene terpolymer; composites

INTRODUCTION

Dynamic vulcanization (DV) means the selective curing of the thermosetting rubber component and its fine dispersion in molten thermoplastic resin via intensive mixing or kneading. This process yields a fine dispersion of partially or fully microsize rubber particles in the thermoplastic matrix.

The dynamically cured thermoplastic elastomer blends, first described by Fischer^{1,2} have been widely used in the plastic industry for years.^{3–5} The blends have important technical advantages in processing because the blends can be fabricated by methods such as extrusion and molding. The thermoplastic blend is known to be composed of a partly gelled elastomer and physically crosslinked plastic and thus exhibits a similar behavior to the thermoplastic IPN (interpenetrating polymer network),⁶ which flow at elevated temperature and yet behaves as a thermoset at use temperature.

The improvement in properties resulting from dynamic vulcanization are reduced permanent set,

improved ultimate mechanical properties, greater resistance to attack by fluids, improved high temperature utility, greater stability of phase morphology in melt, greater melt strength, and more reliable thermoplastic fabricability.⁷ Previously, we have reported the effect of dynamic vulcanization of rubberwood in polypropylene/natural rubber composites.^{8,9}

The introduction of cellulosic material into thermoplastic improves the mechanical properties of thermoplastic composites. Paper sludge, one the cellulosic materials, is a by-product from pulp and paper mills. It is mainly composed of cellulosic and inorganic materials.

This article reports the effect of dynamic vulcanization and dynamic vulcanization plus compatibilizer i.e., Maleated Polypropylene (MAPP) (DVC) on torque development, mechanical properties, water absorption, morphology, and thermal properties of polypropylene/ethylene propylene diene terpolymer/paper sludge (PP/EPDM/PS) composites.

EXPERIMENTAL

Materials

Polypropylene homopolymer used in this study was of injection molding grade, from Titan PP polymers

Correspondence to: H. Ismail (hanafi@eng.usm.my).

TABLE I
Formulation of Unvulcanized (UV), Dynamic Vulcanized (DV), and Dynamic Vulcanized Plus Compatibilizer (DVC) of PP/EPDM/PS Composites

Mate UV	UV	DV	DVC
Polypropylene (PP) (wt %)	50	50	50
Ethylene propylene diene terpolymer (EPDM) (wt %)	50	50	50
Paper sludge (PS) (wt %)	0, 15, 30, 45, 60	0, 15, 30, 45, 60	0, 15, 30, 45, 60
MAPP (wt %)	–	–	3
Curative:			
Zinc oxide (wt %)	5	5	5
Stearic acid (wt %)	2	2	2
CBS ^a (wt %)	2	2	2
TMTD ^b (wt %)	2.5	2.5	2.5
Sulfur (wt %)	1	1	1

Curative system based on wt % of EPDM phase only.

^a *N*-cyclohexyl-2-benzothiazol-2-sulphenamide.

^b Tetramethylthiuram disulfide.

(M) Sdn Bhd, Johor, Malaysia (code 6331) with MFI value of 14.0 g/10 min at 230°C. Ethylene propylene diene monomer, grade Mitsui EPT 3072E was obtained from Luxchem Trading Sdn Bhd., Selangor, Malaysia. MAPP was obtained from Aldrich Chemical Company. Zinc oxide, stearic acid, *N*-cyclohexyl-2-benzothiazol-2-sulfenamide (CBS), tetramethylthiuram disulfide (TMTD), and sulfur were obtained from Bayer (M), Penang. PS, a waste product from paper mills process was obtained from Nibong Tebal Paper Mill Sdn Bhd, Penang, Malaysia. PS was dried in vacuum oven at 80°C for 24 h to make it free from moisture and then grinded to become powder. An Endecotts sieve was used to obtain an average filler sizes of 63 μm (density, 2.2 g/cm³). The formulation for unvulcanized, dynamic vulcanized, and dynamic vulcanized plus compatibilizer (MAPP) PP/EPDM/PS composites used in this study is shown in Table I.

Table II shows the results of semiquantitative analysis of PS used in this study.

Measurement of tensile properties

Tensile properties were determined according to ASTM D 638 using an Instron 3366. Dumb-bell shaped specimens were conditioned at ambient temperature (25 ± 3)°C and relative humidity (30 ± 2)% before testing. A crosshead speed of 50 mm/min was used. An average of five samples was used during the test.

Morphology study

Studies on the morphology of the tensile fracture surface of the composites were carried out using a scanning electron microscope (SEM), model Leica

TABLE II
Semi Quantitative Analysis of Paper Sludge Using X-Ray Fluorescence Spectrometer Rigaku RIX 3000

Component	Wt (%)
Na ₂ O	0.057
MgO	3.0
Al ₂ O ₃	7.1
SiO ₂	10.0
P ₂ O ₅	0.065
SO ₃	0.14
Cl ₂ O	0.19
K ₂ O	0.035
CaO	20.0
TiO ₂	0.11
MnO	0.018
Fe ₂ O ₃	0.19
ZnO	0.017
SrO	0.011
LOI (Organic)	59.0

Cambridge S-360. The fracture ends of specimens were mounted on aluminum stubs and sputter coated with a thin layer of gold to avoid electrostatic charging during examination.

Water absorption test

Three dumb-bell samples used for tensile measurements were used in this study. Water absorption test was carried out according to ASTM standard D 750-95. It involved total immersion of the samples in distilled water at room temperature, i.e., 30°C. All the specimens were previously dried in an oven at 50°C for 24 h and then stored in a dessicator. The water absorption test was determined by weighing the specimens at regular intervals. A Mettler balance type AJ150 was used, with a precision of ± 1 mg. The percentage of water absorption, M_t was calculated by

$$M_t = \frac{W_N - W_d}{W_d} \times 100\% \quad (1)$$

where W_d and W_N are original dry weight and weight after exposure, respectively. The average reading of three samples was taken.

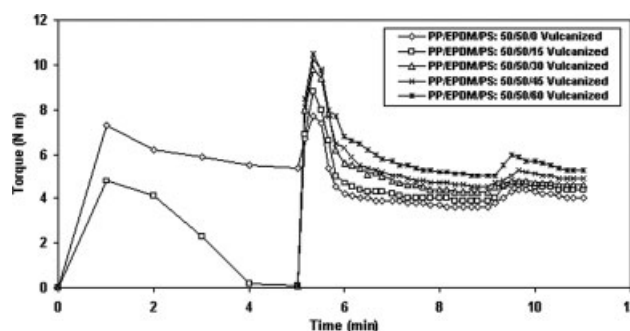


Figure 1 Torque versus time of dynamic vulcanized (DV) of PP/EPDM/PS composites at different filler loading.

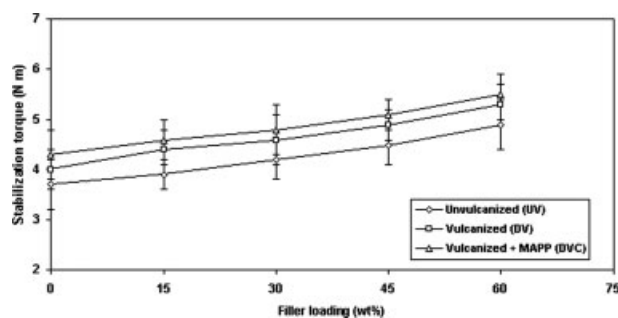


Figure 2 Stabilization torque versus filler loading of unvulcanized (UV), dynamic vulcanized (DV), and dynamic vulcanized plus compatibilizer (DVC) of PP/EPDM/PS composites.

Thermogravimetry analysis

Thermogravimetry analysis of the composites was carried out with a Perkin Elmer Pyris 6 TGA analyzer. The sample weights about 15–25 mg were scanned from 50 to 600°C using a nitrogen air flow of 50 mL/min and a heating rate of 20°C/min. The sample size was kept nearly the same for all tests.

Differential scanning calorimetry

Thermal analysis measurements of selected systems were performed using a Perkin Elmer DSC-7 analyzer. Samples of about 10–25 mg were heated from 20 to 220°C using a nitrogen air flow of 50 mL/min and at a heating rate of 20°C/min. The melting and crystallization behavior of selected composites were also performed using a Perkin Elmer DSC-7. The crystallinity (X_{com}) of composites was determined using the following relationship:

$$X_{com}(\% \text{ crystallinity}) = \Delta H_f / \Delta H_f^0 \times 100 \quad (2)$$

where ΔH_f and ΔH_f^0 are enthalpy of fusion of the system and enthalpy of fusion of perfectly (100%) crystalline PP, respectively. For ΔH_f^0 (PP) a value of

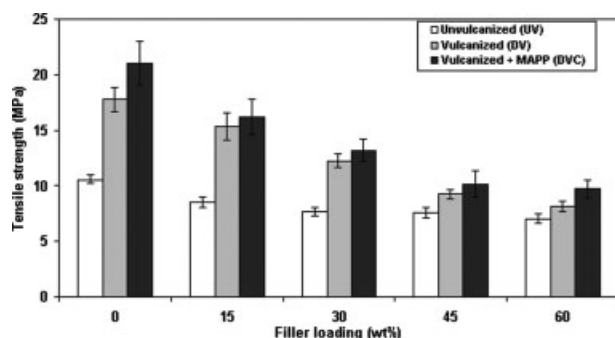


Figure 3 Effect of filler loading on tensile strength of unvulcanized (UV), dynamic vulcanized (DV), and dynamic vulcanized plus compatibilizer (DVC) of PP/EPDM/PS composites.

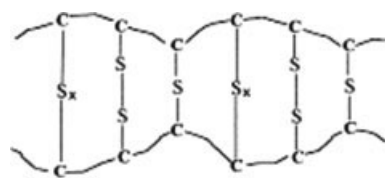


Figure 4 Schematic representation of crosslink formed during dynamic vulcanization using sulfur.¹⁹

209 J/g was used for 100% crystalline PP homopolymer.¹⁰ X_{com} , which is calculated using this equation, however, gives only the overall crystallinity of the composites based on the total weight of composites including noncrystalline fractions, and it is not the true crystallinity of the PP phase. The value of crystallinity for PP phase (X_{pp}) of the PP fraction was normalized using eq. (3) as follow¹¹:

$$X_{pp} = (X_{com}) / W_{f_{pp}} \quad (3)$$

where $W_{f_{pp}}$ is the weight fraction of PP in the composites.

Fourier transform infrared spectroscopy analysis

FTIR spectroscopic analysis of the filler (PS) and composites were carried out in a Perkin Elmer Spectrometer 2000 FTIR. The ATR (Attenuated Total Reflectance) technique and KBr pellet technique were applied. Scanned range was 400–4000 cm^{-1} .

RESULTS AND DISCUSSION

Figure 1 shows the representative torque-time curve for dynamic vulcanized of PS filled polypropylene (PP)/ethylene propylene diene terpolymer (EPDM) composites. (The average reading of three mixing was used). EPDM was charged to the mixing chamber at 0 min and torque was registered, as rotor was not moving. When rotor was started, torque rose due to the resistance created by unmelted EPDM. Upon melting of EPDM, the viscosity decreases. This resulted in lowering the torque. When the filler was

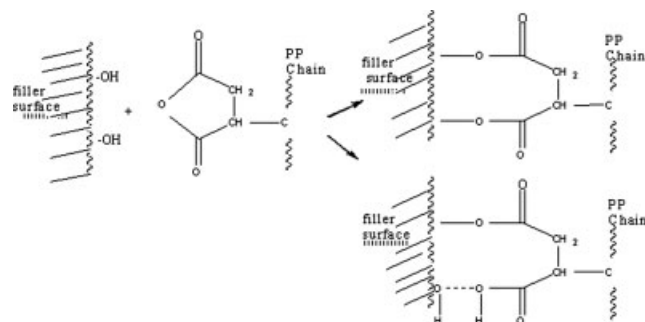


Figure 5 The proposed schematic reaction between filler surface and MAPP in PP/EPDM/PS composites.

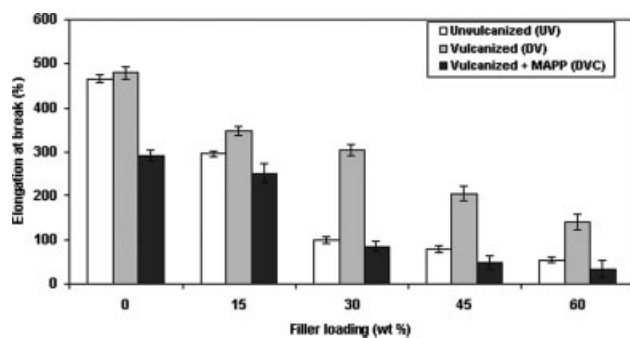


Figure 6 Effect of filler loading on elongation at break of unvulcanized (UV), dynamic vulcanized (DV), and dynamic vulcanized plus compatibilizer (DVC) of PP/EPDM/PS composites.

added at third minute, the torque dropped immediately because PS exists as particles. A similar reduction of torque after the addition of additives such as fillers and curative ingredients has been reported elsewhere.^{12–14} However, torque for dynamic vulcanized at 0 wt % filler loading shows a stable value at third minute. This torque decreases slightly at the fifth minute, due to reduction in viscosity with increase in stock temperature. When unmelted polypropylene was charged into mixing chamber at fifth minute, an abrupt increase in torque was registered. As the polypropylene melted viscosity again tends to decrease due to higher temperature and shear. When curing agents were added at ninth minute, crosslinks were formed which increase the viscosity. The increase of stabilization torque value of dynamic vulcanized (DV) composites after the addition of curative agent indicates that crosslinking and a more stable network structure were formed in the composites.

The stabilization torque values of unvulcanized (UV), dynamic vulcanized (DV), and dynamic vulcanized plus compatibilizer (DVC) of PP/EPDM/PS composites at the end of mixing stage (11 min) were

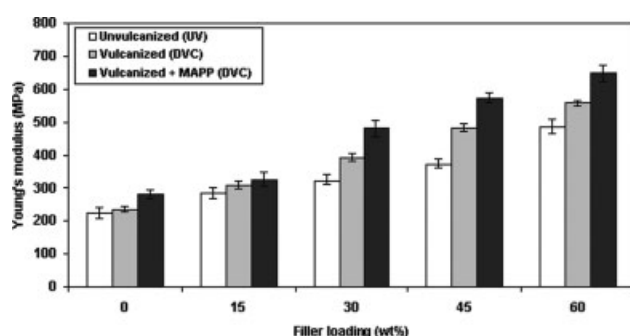


Figure 7 Effect of filler loading on Young's modulus of unvulcanized (UV), dynamic vulcanized (DV), and dynamic vulcanized plus compatibilizer (DVC) of PP/EPDM/PS composites.

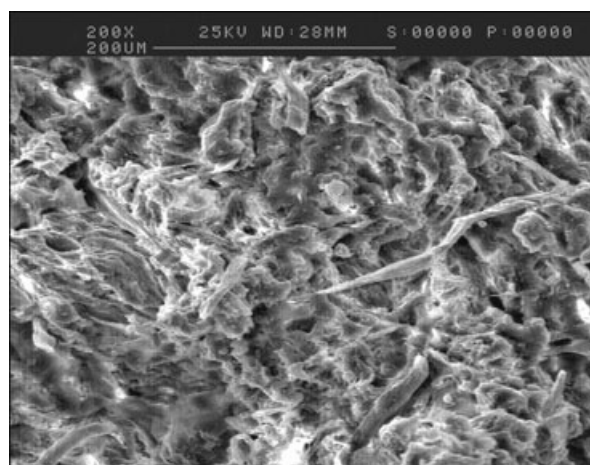


Figure 8 Scanning electron micrograph of tensile fracture surface of unvulcanized (UV) PP/EPDM/PS composite (30 wt %) at magnification of $\times 200$.

plotted versus filler loading as shown in Figure 2. It can be seen that the stabilization torque increases with increasing filler loading. However at a similar filler loading, DVC composites exhibit highest stabilization torque value followed by DV and UV composites. This provides evidence that the formation of crosslink increased the composites viscosity.

The effect of filler loading on tensile strength of PS filled PP/EPDM composites for UV, DV, and DVC is shown in Figure 3. It can be seen that the tensile strength of all composites decrease with increasing filler loading. In our earlier work,¹⁵ we have reported that PS consists of various shape and form such as fiber and particulate. For irregular shape fillers, the tensile strength of the composites decreases due to the inability of the filler to support stresses transferred from matrix.¹⁵ It is clear from Figure 3 that at a similar filler loading, the dynamic vulcan-

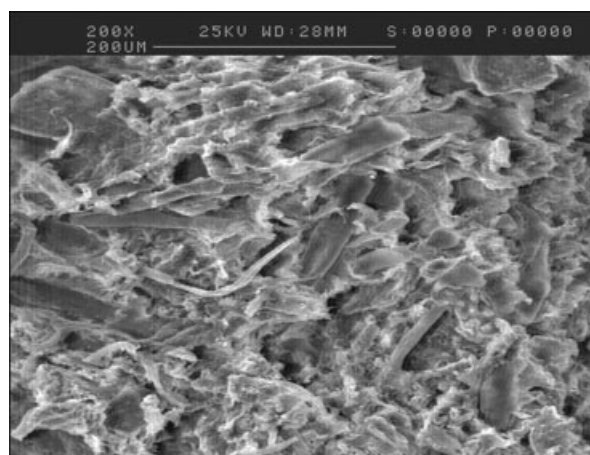


Figure 9 Scanning electron micrograph of tensile fracture surface of unvulcanized (UV) PP/EPDM/PS composite (60 wt %) at magnification of $\times 200$.

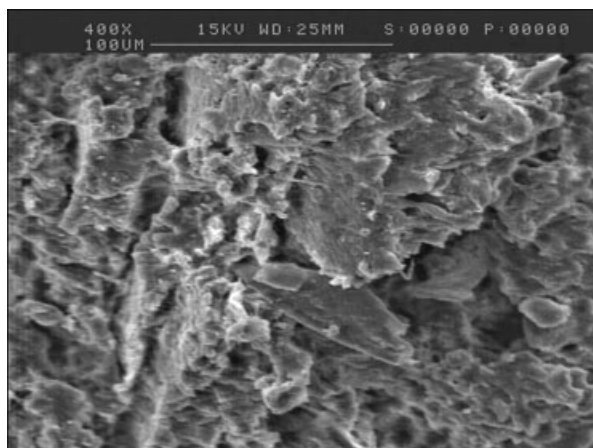


Figure 10 Scanning electron micrograph of tensile fracture surface of dynamic vulcanized (DV) of PP/EPDM/PS composite (30 wt %) at magnification of $\times 200$.

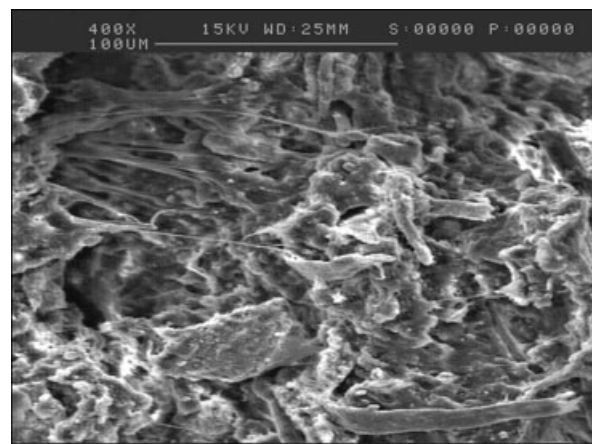


Figure 12 Scanning electron micrograph of tensile fracture surface of dynamic vulcanized plus compatibilizer (DVC) of PP/EPDM/PS composite (30 wt %) at magnification of $\times 200$.

ized (DV) and dynamic vulcanized plus compatibilizer (DVC) composites have better tensile strength than UV composites. The enhanced tensile properties of both vulcanized composites over the unvulcanized counter parts are well explained in the literature for plastic/elastomer blends.^{16–18} Formation of crosslinking in the elastomer phase, which facilitating stresses transfer is the main factor contributing to such enhancements. For DVC composites the highest tensile strength was due to the crosslink formation and the presence of a compatibilizer, MAPP in PP/EPDM/PS composites. A schematic representation of the crosslink formed in EPDM phase during dynamic vulcanization is shown in Figure 4,¹⁹ whereas the proposed compatibilization mechanism formed between PS and PP/EPDM matrix with the presence of MAPP is shown in Figure 5.

The reduction of tensile strength with increasing filler loading indicates the incapability of filler to

support stress transfers from polymer matrix to filler particularly at higher filler loading. This was due to the poor adhesion of filler-matrix and agglomeration of filler particles, as reported in our earlier work.²⁰ At a similar filler loading, DV composites indicate highest elongation at break followed by UV and DVC composites (Fig. 6). The increased of elongation at break of DV composites with increasing filler loading was due to the crosslink formation and better filler dispersion in PP/EPDM matrix which increased the mechanical properties.

Figures 6 and 7 show the effect of filler loading on elongation at break and Young's modulus of UV, DV, and DVC of PP/EPDM/PS composites. At a similar filler loading, DV composites show the highest elongation at break followed by UV and DVC composites. It can be seen that the Young's modulus

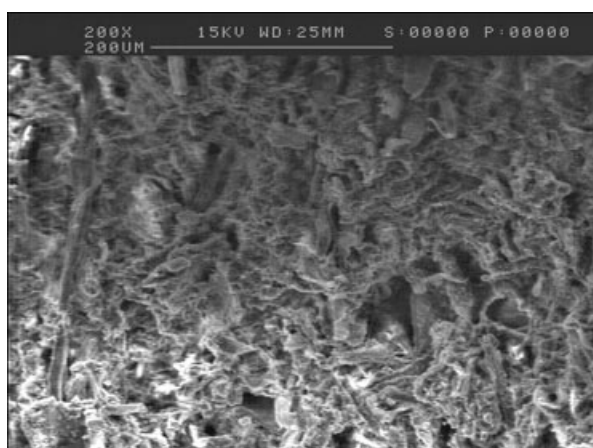


Figure 11 Scanning electron micrograph of tensile fracture surface of dynamic vulcanized (DV) of PP/EPDM/PS composite (60 wt %) at magnification of $\times 200$.

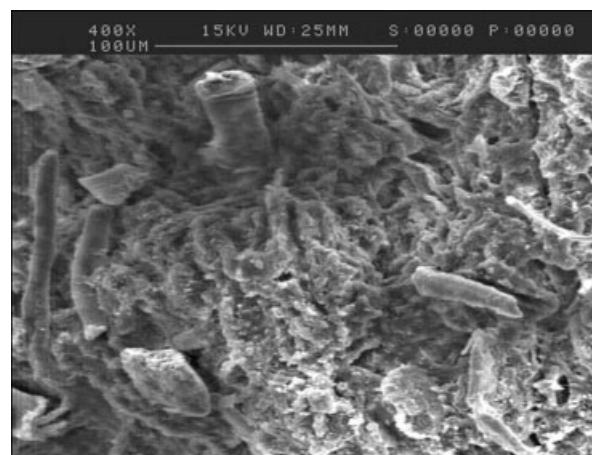


Figure 13 Scanning electron micrograph of tensile fracture surface of dynamic vulcanized plus compatibilizer (DVC) of PP/EPDM/PS composite (60 wt %) at magnification of $\times 200$.

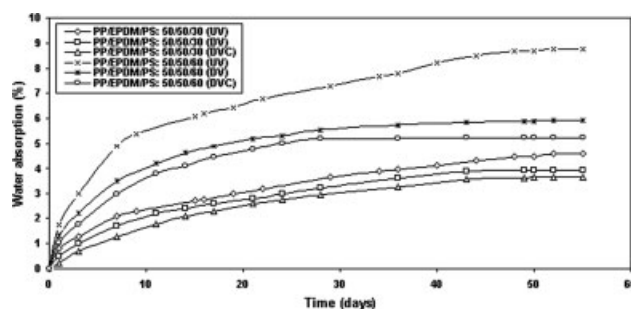


Figure 14 Percentage of water absorption versus time of UV, DV and DVC PP/EPDM/PS composites at different filler loading.

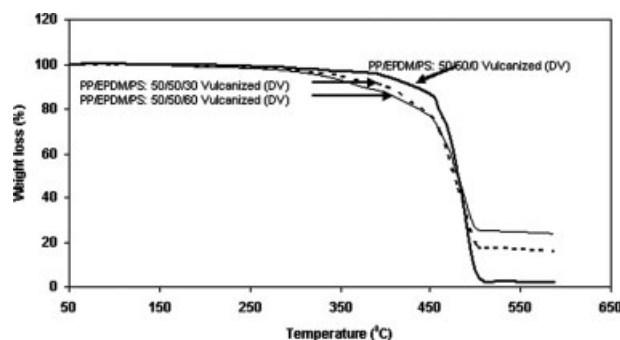


Figure 16 Comparison of thermogravimetric (TGA) analysis curves of dynamic vulcanized (DV) PP/EPDM/PS composites at 0, 30, and 60 wt % of paper sludge.

of all composites increase with increasing filler loading. The Young's modulus of a composite is a measure of the stiffness of the composite. It is determined by taking the slope of the tangent to the curve of the stress-strain curve at zero extension. The addition of PS increases the stiffness of composites. This behavior is consistent with the results reported in our earlier work.²⁰ At a similar filler loading, DVC composites exhibit highest Young's modulus followed by DV and UV composites. The increased of Young's modulus of DVC and DV composites was due to the crosslink formed and the better compatibilization between filler and matrix.

Figures 8 and 9 show the SEM micrograph of the tensile fracture surface of unvulcanized composite at 30 and 60 wt % of PS loading, respectively. It can be seen that both micrographs show unwetted PS on the surface which indicates the poor filler-matrix interaction. Many holes can be seen clearly on the surface due to the detachment of PS from the matrix surface (Figs. 8 and 9). As the amount of filler loading increases, the tendency for filler-filler interaction increases. This results in a higher level of dewetting of PS by the matrix. This explains the lower tensile strength of PP/EPDM/PS composites at higher filler

loading. Figures 10–13 show the SEM micrographs of tensile fracture surfaces of DV and DVC composites at 30 and 60 wt %. It can be seen that these fracture surfaces indicate less PS detachment with matrix tearing particularly in Figure 12. The presence of a crosslink network has enabled the composites to be stretched to greater extent before failure. Figures 10–13 also show that the PSs is well coated by PP/EPDM matrix.

Figure 14 shows the water absorption of PP/EPDM/PS composites for UV, DV, and DVC at 30 and 60 wt % of PS loading. It can be seen that all composites show a similar pattern of water absorption; that is, initial sharp uptake (Fickian absorption behavior) followed by gradual increase until equilibrium water content was achieved at about 50 days. At a similar filler loading, DVC composites indicate a lowest water absorption followed DV and UV composites. This result provides a clear indication of the formation of crosslink density and better interaction between filler and matrix in the DV and DVC composites. As the crosslink density formed in the EPDM phase and compatibilization between filler and PP/EPDM matrix, the composites become stiffer and less penetrable by the water molecules.

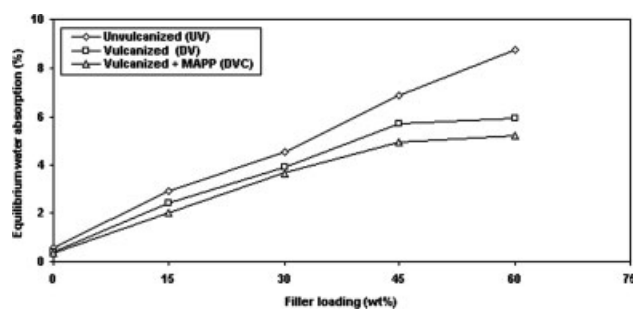


Figure 15 Percentage of equilibrium swelling versus filler loading of unvulcanized (UV), dynamic vulcanized (DV), and dynamic vulcanized plus compatibilizer (DVC) PP/EPDM/PS composites.

TABLE III
Percentage Weight Loss of UV, DV, and DVC PP/EPDM/PS Composites

Composites	T_e (°C)	Total weight loss (%)
PP/EPDM/PS: 50/50/0 (UV)	587.2	100
PP/EPDM/PS: 50/50/30 (UV)	587.4	85.2
PP/EPDM/PS: 50/50/60 (UV)	587.5	76.2
PP/EPDM/PS: 50/50/0 (DV)	588.2	98.1
PP/EPDM/PS: 50/50/30 (DV)	588.3	83.9
PP/EPDM/PS: 50/50/60 (DV)	588.5	74.9
PP/EPDM/PS: 50/50/0 (DVC)	587.4	97.9
PP/EPDM/PS: 50/50/30 (DVC)	587.5	83.9
PP/EPDM/PS: 50/50/60 (DVC)	588.1	75.1

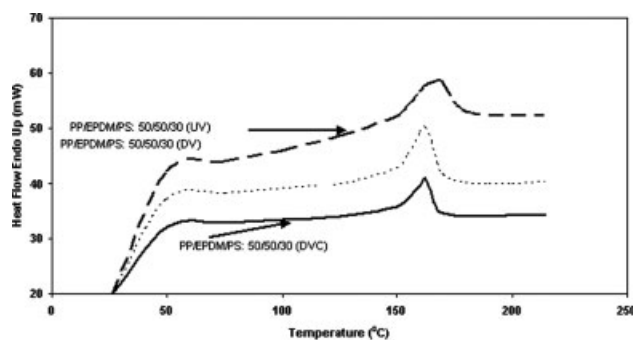


Figure 17 Differential scanning calorimetric (DSC) curves of unvulcanized (UV), dynamic vulcanized (DV), and dynamic vulcanized plus compatibilizer (DVC) of PP/EPDM/PS composites at 30 wt % paper sludge.

Figure 15 shows the equilibrium water absorption for UV, DV and DVC composites at different filler loading. Again at a similar filler loading, DVC and DV composites exhibit lower equilibrium water absorption than UV composites.

Thermogravimetry analysis (TGA) curve of dynamic vulcanized PP/EPDM/PS composites at 0, 30, 60 wt % of PS is shown in Figure 16 and summarized in Table III. It can be seen from Table III that the end degradation temperature (T_e) of composites increases slightly with increasing filler loading. The total weight loss of DV and DVC composites is lower than UV composites. The better thermal stability of DV and DVC composites was due to the presence of inorganic curing agents such as zinc oxide, stearic acid, accelerator, antioxidant, etc.

Figure 17 shows the differential scanning calorimetric (DSC) curves of UV, DV, and DVC PP/EPDM/PS composites at 30 wt % of PS. Table IV indicates the value of melting temperature (T_m), heat of fusion of composites ($\Delta H_{f(\text{com})}$), crystallinity of composites (X_{com}), and crystallinity of PP (X_{pp}) for UV, DV, and DVC plus MAPP of PP/EPDM/PS composites. It can be seen from Table IV that the value of $\Delta H_{f(\text{com})}$ and X_{com} for all composites

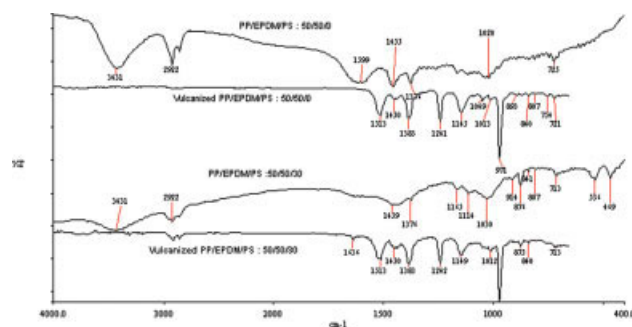


Figure 18 FTIR spectra comparison of unvulcanized and dynamic vulcanized of PP/EPDM/PS composites at 0 and 30 wt % paper sludge. [Color figure can be viewed in the online issue, which is available at www.interscience.wiley.com.]

decreased with increasing PS loading. This was due to the decreasing of PP content with increasing PS loading. Dynamic vulcanized plus MAPP (DVC) composites exhibit the highest value of enthalpy during crystallization process compared to DV and UV composites. The increasing crystallinity of DVC and DV composites was due to the increasing of crosslink and better compatibility between PS and matrix that increased the nucleation activity of PS. However, the melting temperatures of DV and DVC composites exhibit lower values than UV composites.

Figures 18 and 19 show the FTIR spectra comparison of unvulcanized (UV), dynamic vulcanized (DV), and dynamic vulcanized plus compatibilizer (DVC) of PP/EPDM/PS composites at 0, 30 wt % PS. It can be seen that the FTIR of DV and DVC composites exhibit no stretching vibration of —OH at 3431 cm^{-1} compared to UV composites. The introduction of DV and DVC into PP/EPDM/PS composites leads to appearance of two absorption peaks at 1636 and 1242 cm^{-1} . The peak at 1636 cm^{-1} was due to carbonyl group from the addition of chemical curative and compatibilizer (MAPP). The peak at 1242 cm^{-1} indicates the existence of C—O—C group from TMTD curative agent.

TABLE IV
Parameter DSC Data of UV, DV, and DVC PP/EPDM/PS Composites at Different Filler Loading

Composites	Melting temperature T_m (°C)	$\Delta H_{f(\text{com})}$ J/g	X_{com} (% crystallinity)	X_{pp} (%)
PP/EPDM/PS: 50/50/0 (UV)	167.1	40.07	19.2	38.4
PP/EPDM/PS: 50/50/30 (UV)	167.3	36.45	17.4	45.1
PP/EPDM/PS: 50/50/60 (UV)	167.5	35.35	16.9	54.1
PP/EPDM/PS: 50/50/0 (DV)	162.2	42.3	20.2	40.4
PP/EPDM/PS: 50/50/30 (DV)	162.2	38.9	18.6	48.3
PP/EPDM/PS: 50/50/60 (DV)	161.7	36.4	17.4	55.7
PP/EPDM/PS: 50/50/0 (DVC)	162.7	46.9	22.4	44.8
PP/EPDM/PS: 50/50/30 (DVC)	162.1	39.7	19.0	49.4
PP/EPDM/PS: 50/50/60 (DVC)	162.8	37.4	17.9	57.2

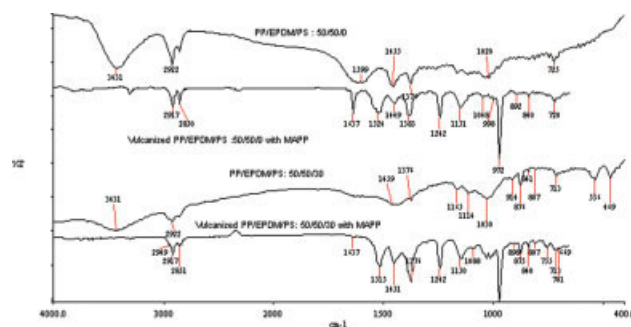


Figure 19 FTIR spectra comparison of unvulcanized and dynamic vulcanized plus compatibilizer of PP/EPDM/PS composites at 0 and 30 wt % paper sludge. [Color figure can be viewed in the online issue, which is available at www.interscience.wiley.com.]

CONCLUSIONS

The dynamic vulcanization (DV) and dynamic vulcanization plus compatibilizer (DVC) of PP/EPDM/PS composites increased the tensile strength, elongation at break (except DVC composites), Young's modulus, and reduced the water absorption of composites. The SEM tensile fracture studies indicate the increase of interfacial interaction between PS and PP/EPDM matrix with dynamic vulcanization and dynamic vulcanization plus compatibilizer. Results from thermal properties also show that DV and DVC increase the thermal stability and crystallinity of PP/EPDM/PS composites.

References

1. Fischer, W. K. U. S. Pat. 3,758,643 (1973).
2. Fischer, W. K. U. S. Pat. 3,862,106 (1975).
3. Coran, A. Y.; Patel, R. *Rubber Chem Technol* 1983, 56, 210.
4. Coran, A. Y.; Patel, R. *Rubber Chem Technol* 1981, 54, 892.
5. Coettler, L. A.; Richwine, J. R.; Wille, F. J. *Rubber Chem Technol* 1982, 55, 1448.
6. Sperling, L. H. *Interpenetrating Polymer Networks and Related Materials*; Plenum: New York, 1981; pp 99–101.
7. George, J.; Varughese, K. T.; Thomas, S. *Polymer* 2000, 41, 1507.
8. Ismail, H.; Salmah, H.; Nasir, M. *Polym Test* 2001, 20, 819.
9. Ismail, H.; Salmah, H.; Nasir, M. *Int J Polym Mater* 2003, 52, 299.
10. Greco, R.; Manacarella, C.; Martuscelli, E.; Ragosta, G. *Polymer* 1987, 28, 1929.
11. Shonaike, G. O.; Kiat, T. H. *J Appl Polym Sci* 1998, 68, 350.
12. Siriwardena, S.; Ismail, H.; Ishiaku, U. S. *Polym Test* 2001, 20, 105.
13. George, K. E.; Joseph, R.; Francis, D. J. *J Appl Polym Sci* 1986, 32, 2867.
14. Mousa, A.; Ishiaku, U. S.; Mohd Ishak, Z. A. *Plast Rubber Compos Proces Appl* 1997, 26, 331.
15. Ismail, H.; Salmah, H.; Bakar, A. A. *J Reinforc Plast Compos* 2005, 24, 147.
16. Gupta, N. K.; Jain, A. K.; Singhal, R.; Nagpal, A. K. *J Appl Polym Sci* 2000, 78, 2104.
17. Sabet, S. A.; Puydak, R. C.; Rader, C. P. *Rubber Chem Technol* 1986, 69, 477.
18. Jain, A. K.; Nagpal, A. K.; Singhal, R.; Gupta, N. K. *J Appl Polym Sci* 2000, 78, 2089.
19. Asaletha, R.; Kumaran, M. G.; Thomas, S. *Eur Polym J* 1999, 35, 253.
20. Siriwardena, S.; Ismail, H.; Ishiaku, U. S.; Perera, M. C. S. *J Appl Polym Sci* 2002, 85, 438.